Current Opinion in Solid State and Materials Science 44 (2026) 101267

Contents lists available at ScienceDirect

Current Opinion in Solid State & Materials Science

journal homepage: www.elsevier.com/locate/cossms

Intracellular microelectrode array (iMEA) and synaptic connectivity mapping

Woo-Bin Jung [a,b,*], Hanju Kim [b], Yoon Ho Jang [b,c], Nadir Talha [b], Hefei Liu [b], Jun Wang [b,d], Donhee Ham [b,*]

[a] Department of Chemical Engineering, Pohang University of Science and Technology, Pohang 37673, South Korea
[b] John A. Paulson School of Engineering and Applied Sciences, Harvard University, Cambridge, MA, USA
[c] Department of Materials Science and Engineering and Inter-university Semiconductor Research Center, College of Engineering, Seoul National University, Seoul 08826, South Korea
[d] Bradley Department of Electrical and Computer Engineering, Virginia Tech, Blacksburg, VA 24061, USA

ARTICLE INFO

Keywords:
Intracellular bioelectronics
Intracellular recording
Massively parallel intracellular recording
CMOS bioelectronics
Microelectrode array (MEA)
Intracellular microelectrode array (iMEA)
Synaptic connectivity
Functional connectivity
Neuromorphic engineering

ABSTRACT

– Intracellular recording offers exquisite access to the electrical interior of a neuron—detecting not only spikes but also the small synaptic signals that reflect synaptic connections and their properties—but it had been limited to only one cell at a time. In 2020, a CMOS nanoelectrode array broke this constraint and massively parallelized intracellular recording, opening a path to capturing synaptic signals across a neuronal network. This shift led us in 2021 to propose the copy framework: population-scale intracellular recording is a process of copying a biological network, because the resulting data—rich with synaptic signals from across the network—reveal its synaptic connectivity map. In this *Perspective*, we revisit that framework because the recent CMOS intracellular microelectrode array (iMEA), building on the 2020 nanoelectrode array, transforms copy from a demanding demonstration into a practical, high-yield technology. By routinely recording intracellular signals across thousands of neurons, the iMEA uncovers synaptic organization with a breadth and clarity previously unreachable. We outline the development of the iMEA as an improved copy platform, what it now enables, and what must still be advanced to build a richer synaptic connectivity map—one that is indispensable to understanding how the brain functions, and provides a firmer foundation for neuromorphic models grounded in the brain's own wiring.

1. Introduction

Despite major progress in artificial solid-state neurons and synapses [1–3], neuromorphic engineering still faces a central barrier: we do not yet possess a practical understanding of how billions of biological neurons and their even more numerous synapses are functionally interconnected. Without such knowledge, we cannot determine how to wire artificial counterparts to reverse-engineer biological computation. Consequently, neuromorphic engineering has gravitated toward abstractions of broad brain properties—such as in-memory and event-driven computing [4–6]—rather than faithful reconstructions of neuronal circuitry.

Our 2021 article in *Nature Electronics* proposed a route to addressing this barrier through what we termed a **copy** framework [7]. Copy refers to massively parallel, high-sensitivity intracellular recordings of a biological neural network, which capture not only action potentials (APs, or spikes) but also much smaller postsynaptic potentials (PSPs), revealing abundant AP-PSP motifs. Since these motifs reflect the physical character of synaptic transmission, copy yields a synaptic connectivity map that not only reconstructs structural connectivity—defining which neurons are connected—but also annotates each identified synaptic connection with its physical properties, such as polarity and strength.

The copy concept in 2021 was motivated by our first demonstration of massively parallel intracellular recordings using a nanoelectrode array in 2020, which enabled the mapping of more than 300 synaptic connections across thousands of neurons, categorized as excitatory or inhibitory [8]. Building directly on this pioneering demonstration, we recently developed the **intracellular microelectrode array (iMEA)** (2025), which represents a substantially improved copy platform that transforms massively parallel intracellular recording into a routine capability (Figs. 1 and 2) [9]. In its initial demonstration, the iMEA recorded intracellular signals from nearly all (~4000) electrodes, from

* Corresponding authors.
E-mail addresses: woobinjung@postech.ac.kr (W.-B. Jung), donhee@seas.harvard.edu (D. Ham).

https://doi.org/10.1016/j.cossms.2026.101267
Received 24 December 2025; Received in revised form 9 March 2026; Accepted 9 April 2026
Available online 21 April 2026

which more than 70,000 plausible synaptic connections were mapped among over 2000 neurons and categorized as excitatory or inhibitory and strong or weak. The scale and content of this map—capturing both structural and physical synaptic organization across the neuronal population—represent an unprecedented advance in synaptic cartography.

The iMEA as an improved copy platform also invites a broader framing: if a functional connectivity map is viewed as stratified into structural, physical synaptic, and higher-order behavioral layers, copy now accesses the first two layers with improved fidelity—the layers that form the basis of behavior—complementing electron microscopy, which primarily accesses the structural layer with ultrahigh anatomical resolution [10–12]. This structural and physical synaptic connectivity map, acquired by copy, offers a foundation for neuromorphic engineering grounded in real biological circuitry rather than abstraction. Given the iMEA development, this *Perspective* revisits the copy framework, reviewing what the iMEA makes possible today and examining where copy must advance next.

2. Population-scale intracellular recording as copy

Achieving both massive parallelism and high-sensitivity intracellular recording had long been a central challenge in neural electrophysiology. On the one hand, the Nobel-prize winning patch-clamp electrode, the gold standard for intracellular recording, resolves both APs and the far smaller PSPs, but is limited to a single neuron at a time. A variety of electrodes of three-dimensional geometries have been explored for intracellular neuronal recording as an alternative to the patch-clamp electrode [13–19], yet most struggled to achieve true intracellular sensitivity to resolve PSPs, and even where such sensitivity was demonstrated, massive parallelism remained out of reach. On the other hand, microelectrode arrays (MEAs) [20,21] represent the mature realization of the parallelism side of the dual challenge, providing stable, long-duration extracellular recordings across large neuronal populations—an indispensable modality for studying long-term network evolution. What MEAs cannot offer, however, is sensitivity to PSPs: their extracellular recording misses PSPs entirely, capturing only APs. Against this backdrop, our nanoelectrode array [8] first combined massive parallelism with intracellular recording, and the iMEA [9] substantially advanced this capability. The iMEA is thus the state-of-the-art copy platform.

2.1. From extracellular to intracellular microelectrode array

MEAs for population-scale extracellular recording and the iMEA for population-scale intracellular recording both are built on CMOS chips containing a large array of active circuits to read and control the electrodes. On this shared CMOS-based architecture, however, the two platforms diverge at the electrode–cell interface (Fig. 1). When a neuron is apposed to an electrode, a thin electrolyte layer—the junctional cleft, filled with the junctional solution—lies between the electrode and the cell membrane. The fluctuation of the membrane potential V_m (*e.g.*, APs, PSPs) inside the neuron propagates across the membrane to modulate the potential V_s in the junctional solution, which is then sensed by the electrode as a voltage V_e. This voltage-transfer, $V_m \rightarrow V_s \rightarrow V_e$, is an attenuation cascade that electrically defines the cell-electrode interface. Minimizing the attenuation in the overall $V_m \rightarrow V_e$ transfer—or, equivalently, maximizing the coupling factor $\alpha \equiv V_e/V_m < 1$—is central to improving the recorded signal quality. This is precisely what distinguishes iMEAs from MEAs: iMEAs have markedly higher α (that is, lower attenuation) than MEAs [9].

There are three attenuation mechanisms associated with the overall voltage-transfer, $V_m \rightarrow V_s \rightarrow V_e$. (see Fig. 1, top right). The first attenuation arises at the neuronal membrane. The membrane forms a barrier between the intracellular space and the junctional cleft, causing a large attenuation in the $V_m \rightarrow V_s$ transfer. The second attenuation is caused by leakage from the junctional solution into the surrounding bulk solution. Seal resistance (R_s) models how effectively the junctional cleft is isolated from the bulk. When R_s is low, voltage changes in the cleft dissipate into the bulk solution, reducing V_s. The third attenuation occurs at the electrode-solution interface in the junctional cleft. This interface has its own impedance Z_e. A larger $|Z_e|$ increases attenuation in the $V_s \rightarrow V_e$ step.

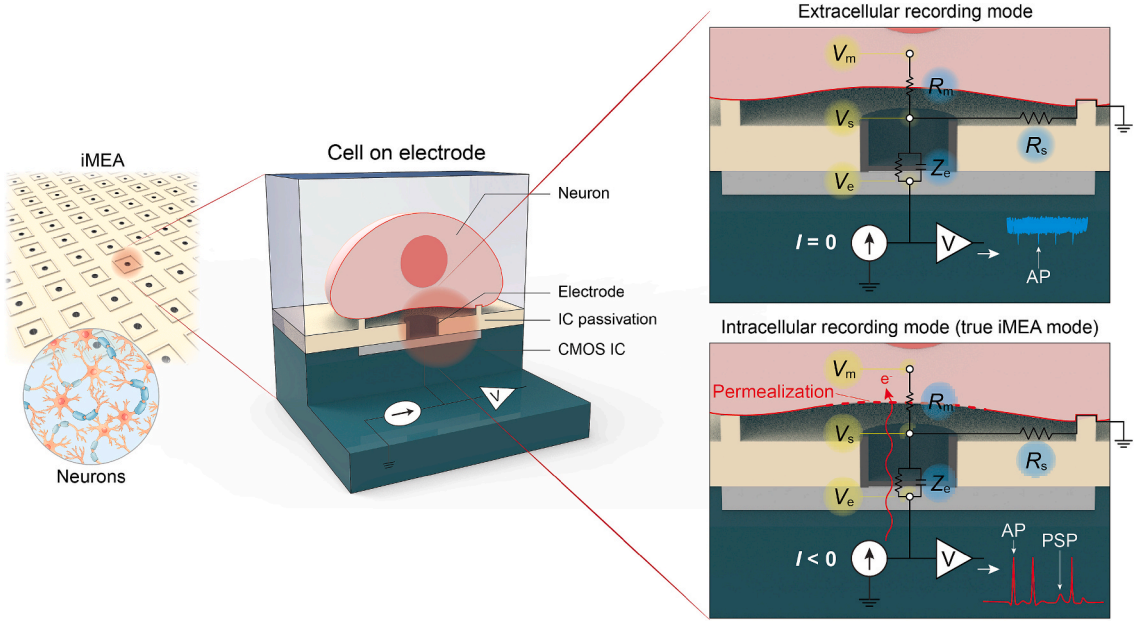

Fig. 1. (Left) Schematic of the intracellular microelectrode array (iMEA) platform and the cell–electrode interface. Each CMOS-integrated microhole electrode is paired with its own current-clamp circuit—comprising a current source and a voltage amplifier—to enable intracellular recording. The electrical circuit model of the cell-electrode interface is shown on the right. (Top right) With current injection turned off, an electrode in the iMEA operates in the conventional extracellular recording mode. The electrode-measured voltage (V_e) is a strongly attenuated version of the membrane potential (V_m), resulting in a low-SNR trace that captures APs but not PSPs. (Bottom right) With current injection turned on during voltage recording, the membrane is permeabilized, allowing the intracellular solution to make more direct contact with the electrode. This markedly increases the coupling strength and recording SNR, revealing not only APs but also PSPs.

Engineering strategies to improve the overall $V_m \rightarrow V_e$ transfer naturally begin with the electrode-solution interface in the junctional cleft (the third attenuation mechanism). Because the interface impedance $|Z_e|$ directly affects the $V_s \rightarrow V_e$ transfer, surface treatments that enlarge the effective electrode area have an immediate impact. Roughening the electrode surface with platinum black (PtB), a widely used approach, increases surface area by at least an order of magnitude [8,9,22], lowering $|Z_e|$ and permitting a far larger fraction of V_s to appear as V_e. Although essential, addressing this third attenuation mechanism is the most straightforward of the three and provides a baseline for improving the overall signal transfer.

A key step in transforming a conventional extracellular MEA into an intracellular platform came from overcoming the membrane-derived attenuation in the $V_m \rightarrow V_s$ transfer (the first attenuation mechanism). In fact, the major credit for this step goes to the 2020 nanoelectrode array [8], the iMEA precursor, which showed that the membrane-derived attenuation can be alleviated by injecting a current during voltage recording. The injected current permeabilizes the membrane, enabling the intracellular solution to make a more direct contact to the electrode, bypassing the membrane. This is intracellular recording. The $V_m \rightarrow V_s$ transfer is still an attenuation but is drastically reduced, increasing the recording signal-to-noise ratio (SNR) by 1 ~ 2 orders of magnitude. This current-clamp intracellular technique records not only APs but also PSPs that are not visible in MEA extracellular recordings.

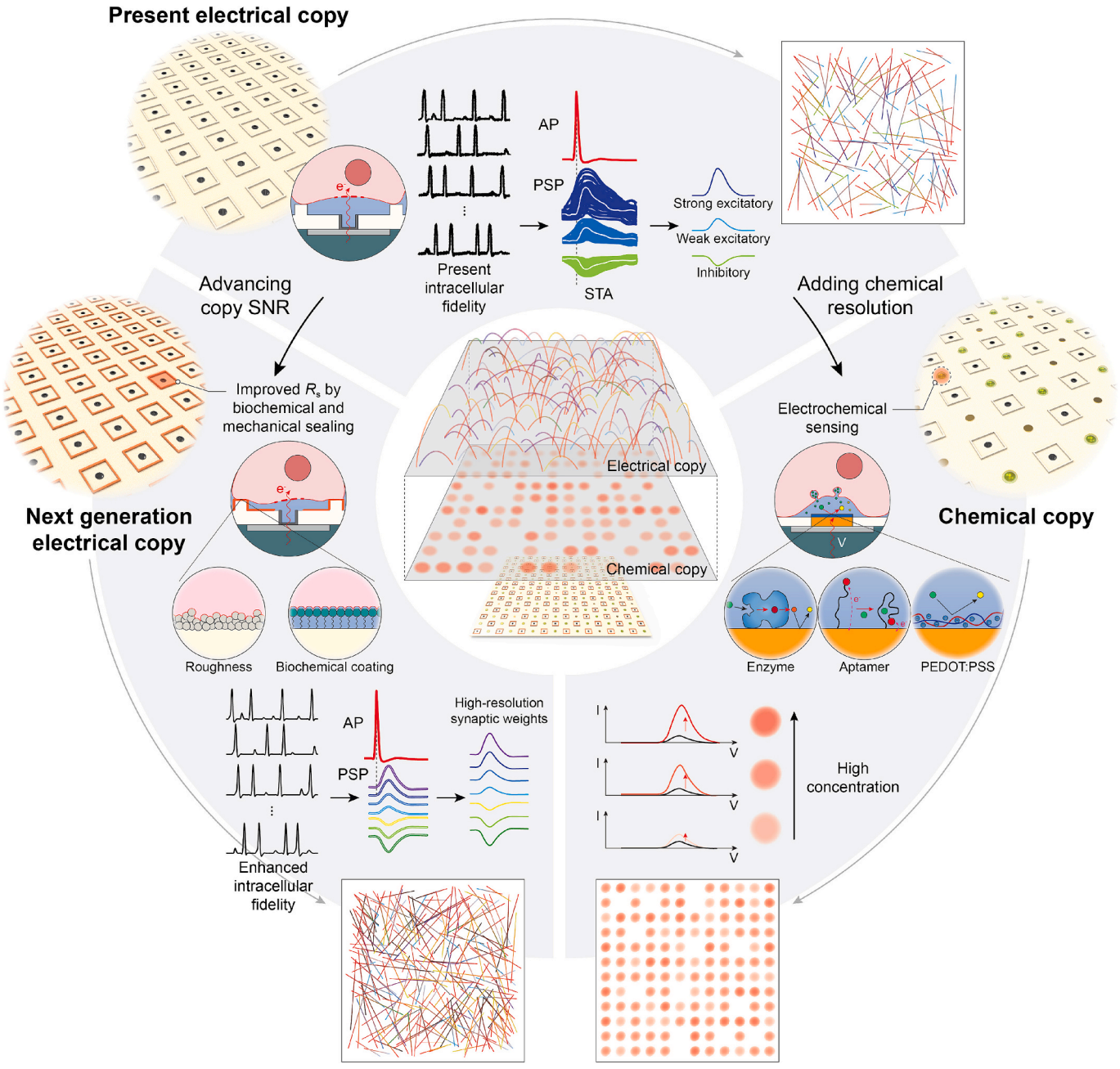

Fig. 2. Conceptual overview of copy. (Top) Present electrical copy refers to massively parallel intracellular recordings with the current iMEA to extract AP–PSP motifs and infer a synaptic connectivity map, but with limited SNR. (Bottom left) Next-generation electrical copy aims to increase intracellular recording SNR through enhanced electrode sealing in an improved iMEA, enabling higher-resolution estimation of synaptic weights. (Bottom right) Future extensions of copy may integrate neurotransmitter-sensing electrodes into the iMEA, combining parallel intracellular electrophysiology with parallel measurements of neurotransmitter release and identity. Incorporating such chemical information would enrich the functional interpretation of synaptic connectivity maps.

The iMEA [9] adopted the same current-clamp strategy from Ref. [8] (Fig. 1, bottom right). In sum, the current-clamp strategy—transforming each electrode from an extracellular observer into a high-sensitivity intracellular probe—established the 2020 nanoelectrode array [8] as the precursor copy platform and provided the foundational mechanism for the 2025 iMEA [9] to become a practical copy platform.

Building on the current-assisted intracellular access demonstrated by the 2020 nanoneedle array, the 2025 iMEA reduced attenuation further by strengthening the seal resistance R_s (the second attenuation mechanism) [9]. Increasing R_s requires the electrode to be fully covered by a neuron. Partial coverage lowers R_s because the electrode remains exposed to both the junctional solution and the surrounding bulk solution, preventing the two regions from being electrically isolated. In population-scale recordings where thousands of electrodes interact with thousands of neurons, the occurrence of full versus partial electrode coverage becomes probabilistic. This makes a small lateral electrode footprint essential for promoting full coverage with high likelihood. At the same time, the electrode must feature sufficient surface area to keep $|Z_e|$ low—since even with PtB, excessively small geometries can still yield a high $|Z_e|$. The microhole electrode resolves this geometric tension (Fig. 1). By recessing the electrode into a small aperture, the microhole provides a compact opening that a single neuron can readily cover, increasing the likelihood of high R_s, while its conductive sidewalls and base provide ample surface area without enlarging the lateral footprint. Indeed the microhole electrode is the hallmark of the 2025 iMEA, converting the current-injection-based intracellular access demonstrated in 2020 into a practical copy platform (Fig. 1).

2.2. Copy with the iMEA

The iMEA is an array of microhole electrodes, each paired with current clamp electronics—a current source circuit that injects a current to permeabilize the membrane above the microhole and an amplifier that records the resulting intracellular voltage [9] (Fig. 1). Thousands of such microhole electrodes then perform parallel intracellular recordings that capture not only APs but also PSPs from across a biological neuronal network. In its first implementation, a 4096-electrode iMEA obtained intracellular signals from nearly all electrodes. These network-wide intracellular signals constitute copy because they contain the information needed to map synaptic connectivity—its structural organization and physical synaptic properties (Fig. 2, top). When two neurons are synaptically connected, an AP in the presynaptic neuron tends to elicit a PSP in the postsynaptic neuron. This AP–PSP pairing is a fundamental electrophysiological motif. Its presence indicates a synaptic connection, while the PSP's shape, amplitude, and probability of occurrence reflect the polarity (excitatory or inhibitory) and the strength—often referred to as weight—of the synaptic connection. A vast number of such AP-PSP pairings populate the iMEA recordings across large neuronal populations, and their detection yields a synaptic connectivity map (Fig. 2, top).

To detect AP-PSP pairings and thus extract connectivity from these recordings, each of the N traces is compared with all other traces, giving $N(N\text{-}1)$ ordered source-target pairs to analyze [9]. In each pair, the source trace is treated as the recording of a potential presynaptic neuron and the target trace as that of a potential postsynaptic neuron. For a given pair, each AP in the source trace provides a temporal anchor. Around each anchor, a short window is opened in the target trace to determine whether a PSP occurs at a consistent latency. Even when individual PSPs are too small to separate from random fluctuations, which is often the case given the current SNR of the iMEA, the windows can be aligned and averaged across repeated anchors, allowing random fluctuations to cancel while consistent PSPs accumulate (Fig. 2, top). This spike-triggered averaging (STA) strategy works for intracellular data, where PSPs are present but can be noisy; in extracellular recordings, PSPs are effectively absent and cannot be revealed by averaging. A clear AP-PSP pairing indicates that the corresponding traces arise from two synaptically connected neurons. Once an AP-PSP pairing is detected, the PSP waveform can be examined to determine the nature of the connection, including its polarity and strength (Fig. 2, top). In this way, synaptic connections and their physical properties emerge from the network-wide intracellular recordings.

Intracellular recordings obtained from nearly all electrodes of the 4,096-electrode iMEA yielded a dataset dense with AP–PSP motifs across thousands of neurons. Applying the analysis described above revealed more than 70,000 plausible synaptic relationships among over 2000 neurons, spanning excitatory or inhibitory, and weak excitatory or strong excitatory connections (Fig. 2, top). This establishes the iMEA-based massively parallel intracellular recording as an improved copy process. Such an outcome had previously been out of reach: intracellular precision had been confined to single-cell patch-clamp recordings, while population coverage had been available only through extracellular MEAs. The 2020 nanoneedle array [8] began to bridge this long-standing divide by demonstrating intracellular recording at population scale, and the iMEA [9] now advances this trajectory by providing practical, higher-yield intracellular recording across populations.

3. Advancing copy

The emergence of the iMEA has turned copy from a conceptual promise into a practical method for reconstructing synaptic connectivity—its structural organization and physical synaptic properties. Yet the current implementation of copy leaves clear frontiers: the intracellular signals the iMEA captures could still improve in SNR to refine the quantitative estimates of synaptic weights, and the neurotransmitter-driven chemical pathways that modulate biological circuit state remain invisible. Copy therefore would be advanced by deepening the iMEA's electrical fidelity to recover synaptic weights with higher precision (Fig. 2, bottom left) and would benefit from expanding the iMEA's chemical scope to annotate each connection with its neurotransmitter identity and modulatory role (Fig. 2, bottom right).

3.1. Improving copy SNR

Further improving the intracellular recording SNR is a central objective for the next generation of iMEA. Although the current iMEA can at times resolve individual PSPs, the cell-electrode coupling factor α varies across electrodes, and a majority of recording traces reveal PSPs only through STA (Fig. 2, top). Such averaging collapses information: it obscures the probability that a PSP occurs following each presynaptic AP, erases the event-to-event variability in PSP amplitude, and prevents accurate measurement of individual PSP waveforms. As a result, synaptic weights can currently be estimated only coarsely—for example, classifying excitatory connections as strong or weak based on averaged waveform morphology rather than quantifying weights on a continuous scale [9] (Fig. 2, top). This low SNR limitation also affects the detection of inhibitory synapses, because inhibitory PSPs (IPSPs) are often smaller in amplitude than excitatory PSPs (EPSPs) in many mammalian circuits. Consequently, inhibitory connections are disproportionately under-detected with the current iMEA with the limited intracellular recording SNR [9]. Improving SNR would thus not only resolve individual PSPs and estimate synaptic weights with much finer granularity, but also uncover a richer inventory of inhibitory connectivity, which is essential for understanding the excitatory–inhibitory balance that governs network dynamics and computation.

The next major frontier for the iMEA is thus the improvement of SNR to approach true patch-clamp levels (Fig. 2, bottom left). Although the iMEA achieves a higher probability in full electrode coverage—a decisive factor behind its high intracellular coupling rate—and elevates R_s as compared to the case of more partial electrode coverage, the full coverage does not guarantee the actual tight seal between the cell membrane and the surface around the electrode, and the true tight sealing would further improve R_s. Patch pipettes obtain high SNR by

mechanically drawing the membrane to form a giga-seal, whereas chip-based interfaces rely on spontaneous membrane–surface apposition, whose tightness and uniformity remain uncontrolled. Future progress will therefore depend on engineering true biochemical and mechanical sealing at the microhole rim and the surrounding well. The microhole and the well together form a nested anchoring geometry analogous to a patch orifice, but adhesion strength must be enhanced through targeted surface chemistry, adhesion-molecule patterning, nanoscale roughness control, and polymer-interface engineering. Such strategies could substantially raise the effective seal resistance, closing the SNR gap with patch-clamp electrophysiology and enabling population-scale intracellular recordings that resolve synaptic weights with much finer granularity, thus allowing for the synaptic cartography with much finer strength annotation (Fig. 2, bottom left).

Even after R_s is substantially improved and individual PSPs become resolvable across the array, the electrode-to-electrode variability in R_s and other interface parameters will remain, leading to corresponding variations in the coupling factor $\alpha = V_e/V_m$— a characteristic of massively parallel intracellular interfaces. Without knowledge of α, the true PSP amplitude inside the neuron, $V_{m,PSP}$, cannot be recovered from the corresponding electrode-measured amplitude, $V_{e,PSP}$, limiting the quantitative interpretation of synaptic weights. This can be addressed by leveraging the biophysical invariance of the AP amplitude inside the neuron. Unlike PSPs, whose amplitudes inside the neuron vary with synaptic strength, the amplitude of an AP within a given neuron type is relatively stereotyped at a known value of $V_{m,AP}$. Accordingly, when an AP appears in the postsynaptic trace, α can be estimated from the AP's electrode-measured amplitude $V_{e,AP}$, since $\alpha = V_{e,AP}/V_{m,AP}$ and $V_{m,AP}$ is known within a narrow physiological range. Once α is determined for a given electrode, $V_{m,PSP}$, the PSP amplitude inside the neuron, can be recovered directly from the PSP's electrode-measured amplitude $V_{e,PSP}$ using the relationship $\alpha = V_{e,PSP}/V_{m,PSP}$. In sum, this AP-mediated calibration determines the electrode-specific coupling factor α, enabling quantitative estimation of PSP amplitudes inside the coupled neuron and, consequently, synaptic weights.

3.2. Adding chemical resolution to copy

The electrical copy—massively parallel intracellular recording of APs and PSPs—can build a synaptic connectivity map by identifying AP–PSP motifs and specifying their strengths and signs. However, such electrical readouts capture only the electrophysiological outcome of synaptic signaling and do not directly report the fast ionotropic neurotransmitter release that mediates these AP–PSP motifs (*e.g.*, glutamate release for excitatory synaptic connections and GABA release for inhibitory synaptic connections) [23]. Direct chemical measurements of neurotransmitters that mediate fast PSPs can thus provide complementary information about release dynamics and local concentration that is not fully specified by PSP amplitude alone. Moreover, many neurotransmitters—including neuromodulators such as dopamine, serotonin and neuropeptides—do not typically manifest as fast PSPs. Their effects unfold over slower timescales and reshape neuronal excitability and plasticity without producing fast PSPs [23]. These modulatory influences therefore lie largely outside the reach of AP-PSP-based copy. In this broader view, enriching copy with broad neurotransmitter information would deepen the functional meaning of synaptic connectivity maps, not only by refining the interpretation of fast synaptic transmission but also by incorporating chemical signaling pathways that are invisible—even indirectly—to purely electrical readouts.

Resolving neurotransmitter release at the single-neuron level—let alone at individual synaptic contacts—remains challenging for electrode-based detection, as release occurs in small volumes. Addressing this frontier has motivated a broad range of chemical-to-electrical transduction strategies in the wider literature, including approaches that functionalize the electrode surface to enhance the transduction. Electrode functionalization with aptamers, enzymes, or conducting polymers such as PEDOT:PSS represents examples of chemical-to-electrical transduction strategies for neurotransmitter sensing [24–26], with the former two approaches providing molecular specificity in addition to transduction. Aptamer interfaces rely on target-induced conformational or charge-distribution changes that translate into shifts in surface potential on the electrode. Enzymatic interfaces, by contrast, generate redox products as the enzyme reacts with neurotransmitters, yielding measurable currents. With conducting polymer coatings such as PEDOT:PSS, neurotransmitter oxidation modulates the polymer's doping state or interfacial potential. At present, these chemical-to-electrical transduction strategies coupled to electrodes have yet to robustly resolve neurotransmitter release at the cellular level.

If and when these challenges are met, electrode-based neurotransmitter sensing modalities can be integrated into the CMOS iMEA platform for parallelism (Fig. 2, bottom right). In such a configuration, intracellular-recording microhole electrodes can be intermixed with functionalized neurotransmitter-sensing electrodes, enabling the same platform to perform both electrical and chemical copy in a complementary manner. This integration is enabled by the fact that the electrical signals—whether surface-potential shifts or redox-generated currents—transduced from chemical activity at the electrode interface are inherently compatible with transistor-based CMOS voltage or current readout architectures (Fig. 2, bottom right), as demonstrated in pioneering proof-of-concept studies such as Ref. [27]. If electrical copy reveals who connects to whom and how strongly, chemical copy would illuminate the connection map with what transmitter, under what modulatory influence, and with what impact on circuit state. This expanded view would move copy closer to capturing the functional grammar of biological neural networks.

4. Conclusion and outlook toward *in vivo* copy

Population-scale intracellular recording grants access to subthreshold synaptic signals across large neuronal assemblies and thus brings the synaptic connectivity of biological neural circuits into view. In this sense, such population-scale intracellular traces constitute a partial copy of the neural circuits—an idea we first articulated in 2021 [7], soon after a CMOS nanoelectrode array first demonstrated massively parallel intracellular recording in 2020 [8]. The CMOS iMEA [9], a new bioelectronic platform building upon that foundational work, routinizes population-scale intracellular recording and thus transforms the copy framework into a practical methodology, opening opportunities across systems neuroscience and providing a firmer foundation for neuromorphic models grounded in real biological circuitry. Enriching the contents of copy—by further increasing intracellular recording SNR to resolve synaptic weights more precisely and by adding chemical copy to identify neurotransmitter classes at cellular resolution—will deepen the interpretive power of the resulting synaptic connectivity maps.

Although population-scale intracellular recording has only recently become feasible *in vitro*—through the development of the CMOS nanoelectrode array in 2020 [8] and its subsequent routinization with the CMOS iMEA in 2025 [9]—extending this capability to the living brain is an entirely different frontier, and achieving population-scale intracellular recording *in vivo* would be transformative.

The immediate question is how to bring the core technology for intracellular recording—microhole electrodes operated by current-clamp electronics—into the living brain. Potential paths forward include two complementary approaches. The first builds on brain-insertable rigid shanks etched as part of a CMOS chip, wherein the shanks embed dense electrode arrays and monolithic interconnects that carry control signals to the electrodes and recorded signals back to the electronics in the chip body. This architecture, underlying platforms such as Neuropixels [28,29], is being widely used for population extracellular recording *in vivo*. Using microhole electrodes in place of the standard electrode geometries and equipping the CMOS chip with current-clamp electronics would constitute a concrete step toward

testing population-scale intracellular recording *in vivo*. The second path builds on flexible or soft, tissue-compliant carriers that embed dense electrode arrays and interconnects [30–35], an approach actively pursued for population-scale extracellular recording *in vivo*. Again replacing the standard electrode geometries with microhole electrodes and linking them to a CMOS chip with current-clamp electronics would constitute an equally concrete step. Both paths can be attempted in the relatively near term, though each involves non-trivial engineering challenges—including managing leakage currents through silicon shanks, which could become more consequential in the current-injection regime of intracellular recording, and establishing robust high-density links between flexible/soft probes and rigid CMOS electronics.

The harder question is whether, once inserted, stable intracellular coupling can be acquired and sustained. Brain micromotion could destabilize the membrane–electrode seal—a concern to which flexible/soft probes are inherently more resilient than rigid shanks. The intracellular interface must also contend with the gradual encapsulation response of glia and immune cells. Whether these cell-electrode interface challenges can be overcome remains an open question. If they can, population-scale intracellular recording *in vivo* would enable the copy framework in the living brain, linking the synaptic connection map with organized behaviors.

Declaration of competing interest

The authors declare that they have no known competing financial interests or personal relationships that could have appeared to influence the work reported in this paper.

Acknowledgements

We gratefully acknowledge the Gates Foundation (INV-089977 to D. Ham) and the Samsung Advanced Institute of Technology (A59707 and A37734 to D. Ham) for supporting research related to this *Perspective*.

Data availability

No data was used for the research described in the article.

References

[1] S. Pazos, K. Zhu, M.A. Villena, O. Alharbi, W. Zheng, Y. Shen, Y. Yuan, Y. Ping, M. Lanza, Synaptic and neural behaviours in a standard silicon transistor, Nature 640 (2025) 69–76, https://doi.org/10.1038/S41586-025-08742-4.

[2] D.B. Strukov, G.S. Snider, D.R. Stewart, R.S. Williams, The missing memristor found, Nature 453 (2008) 80–83, https://doi.org/10.1038/NATURE06932.

[3] Z. Wang, H. Wu, G.W. Burr, C.S. Hwang, K.L. Wang, Q. Xia, J.J. Yang, Resistive switching materials for information processing, Nat. Rev. Mat. 5 (2020) 173–195, https://doi.org/10.1038/s41578-019-0159-3.

[4] P.A. Merolla, J.V. Arthur, R. Alvarez-Icaza, A.S. Cassidy, J. Sawada, F. Akopyan, B. L. Jackson, N. Imam, C. Guo, Y. Nakamura, B. Brezzo, I. Vo, S.K. Esser, R. Appuswamy, B. Taba, A. Amir, M.D. Flickner, W.P. Risk, R. Manohar, D. S. Modha, A million spiking-neuron integrated circuit with a scalable communication network and interface, Science 345 (2014) 668–673, https://doi.org/10.1126/science.1254642.

[5] M.A. Zidan, J.P. Strachan, W.D. Lu, The future of electronics based on memristive systems, Nat. Electron. 1 (2018) 22–29, https://doi.org/10.1038/s41928-017-0006-8.

[6] S. Jung, H. Lee, S. Myung, H. Kim, S.K. Yoon, S.W. Kwon, Y. Ju, M. Kim, W. Yi, S. Han, B. Kwon, B. Seo, K. Lee, G.H. Koh, K. Lee, Y. Song, C. Choi, D. Ham, S. J. Kim, A crossbar array of magnetoresistive memory devices for in-memory computing, Nature 601 (2022) 211–216, https://doi.org/10.1038/S41586-021-04196-6.

[7] D. Ham, H. Park, S. Hwang, K. Kim, Neuromorphic electronics based on copying and pasting the brain, Nat. Electron. 4 (2021) 635–644, https://doi.org/10.1038/S41928-021-00646-1.

[8] J. Abbott, T. Ye, K. Krenek, R.S. Gertner, S. Ban, Y. Kim, L. Qin, W. Wu, H. Park, D. Ham, A nanoelectrode array for obtaining intracellular recordings from thousands of connected neurons, Nat. Biomed. Eng. 4 (2020) 232–241, https://doi.org/10.1038/S41551-019-0455-7.

[9] J. Wang, W. Bin Jung, R.S. Gertner, H. Park, D. Ham, Synaptic connectivity mapping among thousands of neurons via parallelized intracellular recording with a microhole electrode array, Nat. Biomed. Eng. 9 (2025) 1144–1154, https://doi.org/10.1038/S41551-025-01352-5.

[10] S. Dorkenwald, A. Matsliah, A.R. Sterling, P. Schlegel, S. Yu, C.E. McKellar, A. Lin, M. Costa, K. Eichler, Y. Yin, W. Silversmith, C. Schneider-Mizell, C.S. Jordan, D. Brittain, A. Halageri, K. Kuehner, O. Ogedengbe, R. Morey, J. Gager, K. Kruk, E. Perlman, R. Yang, D. Deutsch, D. Bland, M. Sorek, R. Lu, T. Macrina, K. Lee, J. A. Bae, S. Mu, B. Nehoran, E. Mitchell, S. Popovych, J. Wu, Z. Jia, M.A. Castro, N. Kemnitz, D. Ih, A.S. Bates, N. Eckstein, J. Funke, F. Collman, D.D. Bock, G.S.X. E. Jefferis, H.S. Seung, M. Murthy, The FlyWire Consortium, Neuronal wiring diagram of an adult brain, Nature 634 (2024) 124–138, https://doi.org/10.1038/S41586-024-07558-Y.

[11] J.G. White, E. Southgate, J.N. Thomson, S. Brenner, The structure of the nervous system of the nematode, *Caenorhabditis elegans*, Phil. Trans. r. Soc. Lond. b. Biol. Sci. 314 (1986) 1–340, https://doi.org/10.1098/rstb.1986.0056.

[12] L.K. Scheffer, C.S. Xu, M. Januszewski, Z. Lu, S.-y. Takemura, K.J. Hayworth, G.B. Huang, K. Shinomiya, J. Maitlin-Shepard, S. Berg, J. Clements, P.M. Hubbard, W.T. Katz, L. Umayam, T. Zhao, D. Ackerman, T. Blakely, J. Bogovic, T. Dolafi, D. Kainmueller, T. Kawase, K.A. Khairy, L. Leavitt, P.H. Li, L. Lindsey, N. Neubarth, D. J. Olbris, H. Otsuna, E.T. Trautman, M. Ito, A.S. Bates, J. Goldammer, T. Wolff, R. Svirskas, P. Schlegel, E. Neace, C.J. Knecht, C.X. Alvarado, D.A. Bailey, S. Ballinger, J.A. Borycz, B.S. Canino, N. Cheatham, M. Cook, M. Dreher, O. Duclos, B. Eubanks, K. Fairbanks, S. Finley, N. Forknall, A. Francis, G.P. Hopkins, E.M. Joyce, S. Kim, N. A. Kirk, J. Kovalyak, S.A. Lauchie, A. Lohff, C. Maldonado, E.A. Manley, S. McLin, C. Mooney, M. Ndama, O. Ogundeyi, N. Okeoma, C. Ordish, N. Padilla, C.M. Patrick, T. Paterson, E.E. Phillips, E.M. Phillips, N. Rampally, C. Ribeiro, M.K. Robertson, J.T. Rymer, S.M. Ryan, M. Sammons, A.K. Scott, A.L. Scott, A. Shinomiya, C. Smith, K. Smith, N.L. Smith, M.A. Sobeski, A. Suleiman, J. Swift, S. Takemura, I. Talebi, D. Tarnogorska, E. Tenshaw, T. Tokhi, J.J. Walsh, T. Yang, J. A. Horne, F. Li, R. Parekh, P.K. Rivlin, V. Jayaraman, M. Costa, G.S.X.E. Jefferis, K. Ito, S. Saalfeld, R. George, I.A. Meinertzhagen, G.M. Rubin, H.F. Hess, V. Jain, S.M. Plaza, A connectome and analysis of the adult *Drosophila* central brain, eLife 9 (2020) e57443. https://doi.org/10.7554/eLife.57443.

[13] M.E. Spira, A. Hai, Multi-electrode array technologies for neuroscience and cardiology, Nat. Nanotechnol. 8 (2013) 83–94, https://doi.org/10.1038/nnano.2012.265.

[14] N. Shmoel, N. Rabieh, S.M. Ojovan, H. Erez, E. Maydan, M.E. Spira, Multisite electrophysiological recordings by self-assembled loose-patch-like junctions between cultured hippocampal neurons and mushroom-shaped microelectrodes, Sci. Rep. 6 (2016) 27110, https://doi.org/10.1038/srep27110.

[15] R. Liu, R. Chen, A.T. Elthakeb, S.H. Lee, S. Hinckley, M.L. Khraiche, J. Scott, D. Pre, Y. Hwang, A. Tanaka, Y.G. Ro, A.K. Matsushita, X. Dai, C. Soci, S. Biesmans, A. James, J. Nogan, K.L. Jungjohann, D.V. Pete, D.B. Webb, Y. Zou, A.G. Bang, S. A. Dayeh, High density individually addressable nanowire arrays record intracellular activity from primary rodent and human stem cell derived neurons, Nano Lett. 17 (2017) 2757–2764, https://doi.org/10.1021/acs.nanolett.6b04752.

[16] Y. Gu, C. Wang, N. Kim, J. Zhang, T.M. Wang, J. Stowe, R. Nasiri, J. Li, D. Zhang, A. Yang, L.-H.-H. Hsu, X. Dai, J. Mu, Z. Liu, M. Lin, W. Li, C. Wang, H. Gong, Y. Chen, Y. Lei, H. Hu, Y. Li, L. Zhang, Z. Huang, X. Zhang, S. Ahadian, P. Banik, L. Zhang, X. Jiang, P.J. Burke, A. Khademhosseini, A.D. McCulloch, S. Xu, Three-dimensional transistor arrays for intra- and inter-cellular recording, Nat. Nanotechnol. 17 (2022) 292–300, https://doi.org/10.1038/s41565-021-01040-w.

[17] Z.C. Lin, C. Xie, Y. Osakada, Y. Cui, B. Cui, Iridium oxide nanotube electrodes for sensitive and prolonged intracellular measurement of action potentials, Nat. Commun. 5 (2014) 3206, https://doi.org/10.1038/ncomms4206.

[18] X. Duan, R. Gao, P. Xie, T. Cohen-Karni, Q. Qing, H.S. Choe, B. Tian, X. Jiang, C. M. Lieber, Intracellular recordings of action potentials by an extracellular nanoscale field-effect transistor, Nat. Nanotechnol. 7 (2012) 174–179, https://doi.org/10.1038/nnano.2011.223.

[19] C. Xie, Z. Lin, L. Hanson, Y. Cui, B. Cui, Intracellular recording of action potentials by nanopillar electroporation, Nat. Nanotechnol. 7 (2012) 185–190, https://doi.org/10.1038/nnano.2012.8.

[20] M. Schröter, F. Cardes, C.-V.-H. Bui, L.D. Dodi, T. Gänswein, J. Bartram, L. Sadiraj, P. Hornauer, S. Kumar, M. Pascual-Garcia, A. Hierlemann, Advances in large-scale electrophysiology with high-density microelectrode arrays, Lab Chip 25 (2025) 4844–4885, https://doi.org/10.1039/D5LC00058K.

[21] U. Frey, J. Sedivy, F. Heer, R. Pedron, M. Ballini, J. Mueller, D. Bakkum, S. Hafizovic, F.D. Faraci, F. Greve, K.-U. Kirstein, A. Hierlemann, Switch-matrix-based high-density microelectrode array in CMOS technology, IEEE J. Solid-State Circuits 45 (2010) 467–482, https://doi.org/10.1109/JSSC.2009.2035196.

[22] J. Abbott, T. Ye, K. Krenek, L. Qin, Y. Kim, W. Wu, R.S. Gertner, H. Park, D. Ham, The Design of a CMOS Nanoelectrode Array with 4096 Current-Clamp/Voltage-Clamp Amplifiers for Intracellular Recording/Stimulation of Mammalian Neurons, IEEE J. Solid-State Circuits 55 (2020) 2567–2582, https://doi.org/10.1109/JSSC.2020.3005816.

[23] E.R. Kandel, J.H. Schwartz, T.M. Jessell, S.A. Siegelbaum, A.J. Hudspeth, Principles of Neural Science, sixth ed., McGraw-Hill, New York, 2021.

[24] S.T. Keene, C. Lubrano, S. Kazemzadeh, A. Melianas, Y. Tuchman, G. Polino, P. Scognamiglio, L. Cinà, A. Salleo, Y. van de Burgt;, F. Santoro, A biohybrid synapse with neurotransmitter-mediated plasticity, Nat. Mater. 19 (2020) 969–973, https://doi.org/10.1038/s41563-020-0703-y.

[25] C. Zhao, K.M. Cheung, I.-W. Huang, H. Yang, N. Nakatsuka, W. Liu, Y. Cao, T. Man, P.S. Weiss, H.G. Monbouquette, A.M. Andrews, Implantable aptamer-field-effect transistor neuroprobes for in vivo neurotransmitter monitoring, Sci. Adv. 7 (2021) abj7422, https://doi.org/10.1126/sciadv.abj7422.

[26] Y. Ou, A.M. Buchanan, C.E. Witt, P. Hashemi, Frontiers in electrochemical sensors for neurotransmitter detection: towards measuring neurotransmitters as chemical

diagnostics for brain disorders, Anal. Methods 11 (2019) 2738–2755, https://doi.org/10.1039/C9AY00055K.

[27] V. Viswam, J. Dragas, A. Shadmani, Y. Chen, A. Stettler, J. Müller, A. Hierlemann, Multi-functional microelectrode array system featuring 59,760 electrodes, 2048 electrophysiology channels, impedance and neurotransmitter measurement units, Proc. IEEE Int. Solid-State Circuits Conf. (ISSCC) (2016) 394–396, https://doi.org/10.1109/ISSCC.2016.7418073.

[28] J.J. Jun, N.A. Steinmetz, J.H. Siegle, D.J. Denman, M. Bauza, B. Barbarits, A.K. Lee, C.A. Anastassiou, A. Andrei, Ç. Aydın, M. Barbic, T.J. Blanche, V. Bonin, J. Couto, B. Dutta, S.L. Gratiy, D.A. Gutnisky, M. Häusser, B. Karsh, P. Ledochowitsch, C. M. Lopez, C. Mitelut, S. Musa, M. Okun, M. Pachitariu, J. Putzejs, P.D. Rich, C. Rossant, W.-L. Sun, K. Svoboda, M. Carandini, K.D. Harris, C. Koch, J. O'Keefe, T.D. Harris, Fully integrated silicon probes for high-density recording of neural activity, Nature 551 (2017) 232–236, https://doi.org/10.1038/nature24636.

[29] N.A. Steinmetz, Ç. Aydın, A. Lebedeva, M. Okun, M. Pachitariu, M. Bauza, M. Beau, J. Bhagat, C. Böhm, M. Broux, S. Chen, J. Colonell, R.J. Gardner, B. Karsh, F. Kloosterman, D. Kostadinov, C. Mora-Lopez, J. O'Callaghan, J. Park, J. Putzejs, B. Sauerbrei, R.J.J. van Daal, A.Z. Vollan, S. Wang, M. Welkenhuysen, Z. Ye, J. T. Dudman, B. Dutta, A.W. Hantman, K.D. Harris, A.K. Lee, E.I. Moser, J. O'Keefe, A. Renart, K. Svoboda, M. Häusser, S. Haesler, M. Carandini, T.D. Harris, Neuropixels 2.0: a miniaturized high-density probe for stable, long-term brain recordings, Science 372 (2021) eabf4588, https://doi.org/10.1126/science.abf4588.

[30] E. Musk, Neuralink, An integrated brain-machine interface platform with thousands of channels, J. Med. Internet Res. 21 (2019) e16194, https://doi.org/10.2196/16194.

[31] J. Liu, T.-M. Fu, Z. Cheng, G. Hong, T. Zhou, L. Jin, M. Duvvuri, Z. Jiang, P. Kruskal, C. Xie, Z. Suo, Y. Fang, C.M. Lieber, Syringe-injectable electronics, Nat. Nanotechnol. 10 (2015) 629–636, https://doi.org/10.1038/nnano.2015.115.

[32] A. Zhang, E.T. Mandeville, L. Xu, C.M. Stary, E.H. Lo, C.M. Lieber, Ultraflexible endovascular probes for brain recording through micrometer-scale vasculature, Science 381 (2023) 306–312, https://doi.org/10.1126/science.adh391.

[33] Y. Liu, J. Liu, S. Chen, T. Lei, Y. Kim, S. Niu, H. Wang, X. Wang, A.M. Foudeh, J.-B.-H. Tok, Z. Bao, Soft and elastic hydrogel-based microelectronics for localized low-voltage neuromodulation, Nat. Biomed. Eng. 3 (2019) 58–68, https://doi.org/10.1038/s41551-018-0335-6.

[34] P. Le Floch, S. Zhao, R. Liu, N. Molinari, E. Medina, H. Shen, Z. Wang, J. Kim, H. Sheng, S. Partarrieu, W. Wang, C. Sessler, G. Zhang, H. Park, X. Gong, A. Spencer, J. Lee, T. Ye, X. Tang, X. Wang, K. Bertoldi, N. Lu, B. Kozinsky, Z. Suo, J. Liu, 3D spatiotemporally scalable in vivo neural probes based on fluorinated elastomers, Nat. Nanotechnol. 19 (2024) 319–329, https://doi.org/10.1038/s41565-023-01545-6.

[35] N. Li, S. Kang, Z. Liu, S. Wai, Z. Cheng, Y. Dai, A. Solanki, S. Li, Y. Li, J. Strzalka, M. J.V. White, Y.-H. Kim, B. Tian, J.A. Hubbell, S. Wang, Immune-compatible designs of semiconducting polymers for bioelectronics with suppressed foreign-body response, Nat. Mater. (2025), https://doi.org/10.1038/s41563-025-02213-x.